

Impact damage of carbon fiber polymer–matrix composites, studied by electrical resistance measurement

Shoukai Wang^a, D.D.L. Chung^{a,*}, Jaycee H. Chung^b

^aComposite Materials Research Laboratory, University at Buffalo, State University of New York, Buffalo, NY 14260-4400, USA

^bGlobal Contour Ltd, 1145 Ridge Road West, Rockwall, TX 75087, USA

Received 24 June 2004; revised 20 February 2005; accepted 24 February 2005

Abstract

Drop impact damage of continuous carbon fiber epoxy–matrix composite laminates, was studied by electrical resistance measurement, which was shown to be more sensitive than the ultrasonic method. The oblique resistance at an angle between the longitudinal and through-thickness directions was more effective than the surface longitudinal resistance in indicating damage, particularly interior damage. The oblique resistance values from longitudinal segments of a specimen were not additive, but the surface resistance values were. In the case of a unidirectional composite, electrical contacts at 45° from the longitudinal direction in the plane of the laminate were more effective than those at 90°. Even minor damage associated with negligible indentation was sensed. The spatial distribution of damage was also studied.

© 2005 Elsevier Ltd. All rights reserved.

Keywords: A. Carbon fibre; A. Smart materials; B. Electrical properties; D. Non-destructive testing; Damage

1. Introduction

Impact is a commonly encountered cause of damage of structural composites such as polymer–matrix composites containing continuous carbon fibers. Evaluation of impact damage has been conducted in prior work after damage application by ultrasonic inspection [1,2], microscopy [3–5], X-radiography [6] and residual strength measurement [1]. Some of the techniques, such as residual strength measurement, are destructive. Study of the impact damage process has also been conducted in prior work during damage affliction by measurements of strain, stress, fracture toughness and Charpy impact fracture energy [7–12]. In contrast, this paper uses electrical resistance measurement, which is non-destructive, to evaluate impact damage after damage affliction. Although, resistance measurement has been used in prior work to monitor damage during static and fatigue loading [13–18], it has not been previously used to monitor impact damage.

Prior work conducted during static or fatigue loading was restricted to tensile or compressive loading [13–18], which

was associated with damage throughout the cross-section of a specimen. In the case of drop impact, the damage is non-uniformly distributed in the cross section of the specimen. Electrical resistance measurement is shown in this work to be effective for sensing drop impact damage and for distinction between the damage on the two opposite sides of the specimen.

Prior work conducted during static or fatigue loading was restricted to the measurement of the volume resistance [13–18], which relates to the condition of the entire cross section. In contrast, this work involves measurement of the surface resistance and the oblique resistance. The surface resistance refers to the resistance of the surface region as measured by using four electrical contacts (A_1 and A_4 for current; A_2 and A_3 for voltage) that are all located on the same surface (Fig. 1). The oblique resistance refers to the resistance in a direction that is between the in-plane and through-thickness directions, as measured by using two electrical contacts (one for current and one for voltage) on each of the two opposite surfaces, such that the contacts on the two surfaces are not directly opposite. For example, the oblique resistance in the direction from A_1 to B_2 in Fig. 1 may be measured by using A_1 and B_2 as current contacts and A_2 and B_1 as voltage contacts.

The through-thickness resistance is sensitive to delamination, while the surface resistance is more sensitive to fiber breakage. Measurement of the through-thickness resistance

* Corresponding author. Tel.: +716 645 2593 Ext:2243; fax: +716 645 3875.

E-mail address: ddlchung@buffalo.edu (D.D.L. Chung).

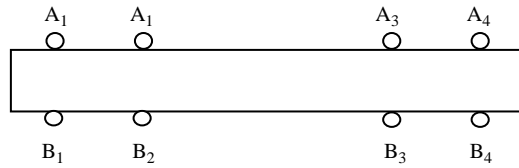


Fig. 1. Schematic of the edge of a composite to illustrate the concept behind the placement of electrical contacts. A_1, A_2, A_3, A_4 are contacts on one surface; B_1, B_2, B_3 and B_4 are contacts on the opposite surface. All the contacts are strips of about 2 mm wide in the direction perpendicular to the length of the composite.

involves two contacts on each of the two opposite surfaces, such that the contacts on the two surfaces are directly opposite. For example, the through-thickness resistance in the direction from A_3 to B_3 in Fig. 1 may be measured by using A_3 and B_3 as current contacts and A_4 and B_4 as voltage contacts, provided that A_3 and A_4 are closely spaced and B_3 and B_4 are closely spaced. However, a better configuration for measuring the through-thickness resistance involves the current contact in the form of a loop and the voltage contact on the same surface in the form of a dot at the center of the loop [14].

The contact configuration for measurement of the oblique resistance is less restrictive than that for measurement of the through-thickness resistance, since the contacts on the two sides do not need to be directly opposite. Therefore, oblique resistance measurement is easier to implement on structural composite components, the shape of which may make it difficult to have electrical contacts that are directly opposite on the two sides. Moreover, the oblique resistance is sensitive to both delamination and fiber breakage, so it may provide a good indication of the overall level of damage. This paper provides, the first investigation of the use of the oblique resistance to indicate damage in composites.

The use of a total of four electrical contacts is in accordance with the four-probe method of electrical resistance measurement. This method is more reliable than the two-probe method, due to the essential elimination of the contact resistance from the measured resistance [19].

Resistance measurement is not a conventional method of damage detection. One of the most effective conventional methods is ultrasonic inspection (the pulse echo method). This paper provides, a comparison of the effectiveness of the resistance and ultrasonic methods by applying both methods to the same damaged specimen.

This paper is aimed at (i) demonstrating the feasibility of DC electrical resistance measurement for assessing the impact damage of carbon fiber epoxy–matrix composites, (ii) investigating the effectiveness of the oblique resistance and of the surface resistance for indicating damage in such composites, and (iii) comparing the effectiveness of the resistance and ultrasonic methods for composite damage detection.

2. Experimental methods

Commercially manufactured composites in the form of continuous carbon fiber epoxy–matrix laminates were cut into strips of size $200 \times 10 \text{ mm}^2$. The length of 200 mm was limited by the size of the steel block at the base of the drop impact instrument. The width of 10 mm was chosen to provide a substantial resistance of the specimen in the longitudinal direction and to avoid the edge effect. That the edge effect was negligible is shown by the absence of observable change at the edge before and after impact. Each strip was sanded by using 600 grit silicon carbide sand paper for the purpose of removing the surface layer (about $20 \mu\text{m}$ thick) of epoxy matrix prior to the application of electrical contacts. The contacts were in the form of silver paint in conjunction with copper wire. The sanding step is not essential, but it helps the electrical measurement by increasing the accuracy and decreasing the noise. Although, the entire surface was sanded in this work, only the portions beneath the electrical contacts needed to be sanded.

Three types of laminate were studied, namely an eight-lamina quasi-isotropic $[0/45/90/-45]_s$ laminate (thickness = 1.0 mm), an eight-lamina unidirectional $[0]_8$ laminate (thickness = 1.0 mm), and a 24-lamina quasi-isotropic $[0/45/90/-45]_{3s}$ laminate (thickness = 3.2 mm).

For the eight-lamina quasi-isotropic composite, four electrical contacts were applied on each of the two sides. Each contact was in the form of a line along the 10-mm width of the specimen, as shown in Fig. 2. The point of impact was at the center along the specimen length.

For the eight-lamina unidirectional composite, four electrical contacts were applied on the top side (impact side) of the specimen only. Each contact was in the form of a line at an angle of 45° from the length of the specimen, as shown in Fig. 3. The 45° orientation of the contacts allows the current to have a minor component that is in the transverse direction. This component is valuable, because the damage in the unidirectional composite involves mainly the cracking of the matrix between the fibers.

For the purpose of comparison between the effectiveness of contacts directed at 45° from the length of the specimen and that of contacts directed at 90° from the length of

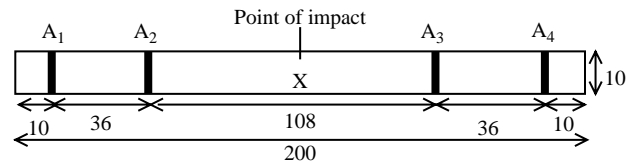


Fig. 2. Eight-lamina quasi-isotropic composite specimen testing configuration (top view). A_1 and A_4 are current contacts; A_2 and A_3 are voltage contacts. Contacts A_1, A_2, A_3 and A_4 are on only the top side of the specimen. Contacts B_1, B_2, B_3 and B_4 (not shown) are on the opposite side, such that B_1 is directly opposite A_1 , B_2 is directly opposite A_2 , B_3 is directly opposite A_3 , and B_4 is directly opposite A_4 . The point of impact is at the center of the specimen along its 200-mm length. All dimensions are in mm.

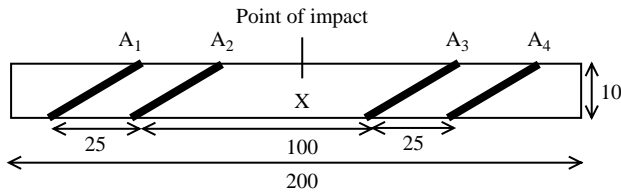


Fig. 3. Eight-lamina unidirectional composite testing configuration (top view). Contacts A_1 , A_2 , A_3 and A_4 are parallel to one another on only the top side of the specimen. They are symmetrically located relative to the center of the specimen (indicated by X). A_1 and A_4 are current contacts; A_2 and A_3 are voltage contacts. Each contact is at an angle of 45° relative to the length of the specimen. The point of contact is at the center. All dimensions are in mm.

the specimen, the unidirectional composite was also tested using the 90° contacts, as shown in Fig. 4.

For the 24-lamina quasi-isotropic laminate, six electrical contacts were applied on each of two sides. Six contacts rather than four contacts were used in order to obtain information of the spatial distribution of damage. Each contact was in the form of a line along the 10-mm width of the specimen, as shown in Figs. 5 and 6.

DC electrical resistance measurement was conducted using the four-probe method. A Keithley 2002 multimeter was used. In the case of the eight-lamina quasi-isotropic composite (Fig. 2), the surface resistance of the top side was measured by using A_1 and A_4 as current contacts and A_2 and A_3 as voltage contacts; the surface resistance of the bottom side was measured by using B_1 and B_4 as current contacts and B_2 and B_3 as voltage contacts; the oblique resistance was measured using A_1 and B_4 as current contacts and A_2 and B_3 as voltage contacts. In the case of the eight-lamina unidirectional composite (Fig. 3), the surface resistance of the top side was measured by using A_1 and A_4 as current contacts and A_2 and A_3 as voltage contacts.

In the case of the 24-lamina quasi-isotropic composite (Fig. 5), the surface resistance of the top side was measured by using A_1 and A_6 as current contacts, together with (i) A_2 and A_5 as voltage contacts for measuring the resistance of the segment ($L+M+R$ in Fig. 5) between A_2 and A_5 , (ii) A_3 and A_4 as voltage contacts for measuring the resistance of the middle segment (shaded and labeled M in Fig. 5), (iii) A_2 and A_3 as voltage contacts for measuring the resistance of the left segment (shaded and labeled L in Fig. 5), or (iv) A_5 and A_6 as voltage contacts for measuring the resistance of the right

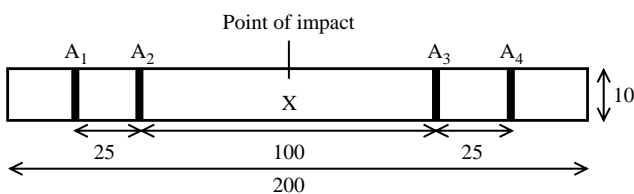


Fig. 4. Eight-lamina unidirectional composite specimen testing configuration (top view). A_1 and A_4 are current contacts; A_2 and A_3 are voltage contacts. All four contacts are on only the top side of the specimen. All dimensions are in mm.

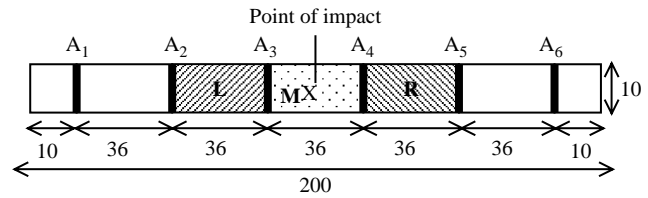


Fig. 5. 24-Lamina quasi-isotropic composite testing configuration (top view). Contacts A_1 , A_2 , ..., A_6 are on the top side. Contacts B_1 , B_2 , ..., B_6 (not shown) are on the bottom side. All dimensions are in mm.

segment (shaded and labeled R in Fig. 5). Corresponding contacts B_1 , B_2 , ..., B_6 (not shown in Fig. 5) on the bottom side were similarly used for measuring the surface resistance of the segments at the bottom side. For measuring the oblique resistance, A_1 and B_6 were used as current contacts; (i) A_2 and B_5 were used as voltage contacts for measuring the oblique resistance of the segment ($L+M+R$) between A_2 and B_5 , (ii) A_3 and B_4 were used as voltage contacts for measuring the oblique resistance of the middle segment, (iii) A_2 and B_3 were used as voltage contacts for measuring the oblique resistance of the left segment, and (iv) A_4 and B_5 were used as voltage contacts for measuring the oblique resistance of the right segment. Thus, the configuration of Fig. 5 allowed damage sensing in the region away from the point of impact, as well as the region containing the point of impact.

Before, during and after impact using a steel hemisphere (19 mm or 0.75 in diameter) dropped from a controlled height, resistance measurement was made. For the case of spatial distribution study, resistance measurement at a given location of a specimen was made before and after impact, but not during impact. The impact energy was calculated from the weight of the ball assembly (either 0.698 or 0.740 kg) and the initial height of the ball (up to 850 mm). The impact was directed at the same point of the specimen at progressively increasing energy. Hence, the cumulative damage was analyzed. Although cumulative damage is more than damage resulting from a single impact at the maximum impact energy used in inflicting cumulative damage, it is meaningful in providing the damage evolution for the same specimen as the impact energy progressively increased. The use of a different specimen for each impact energy, as needed for single impact damage study, was involved in this work to a limited extent.

The damage resulted in an indentation in the shape of a shallow bowl, the diameter of which was measured by using calipers in order to provide a rough indication of the extent of damage. The depth of the indentation was too small for accurate measurement, so it was calculated from the diameter of the indentation and the diameter of the impacting hemisphere. This rough indication was then correlated with the indication provided by electrical resistance measurement.

Multiple specimens of each type were similarly tested by resistance measurement in order to ascertain the reproducibility of the results.

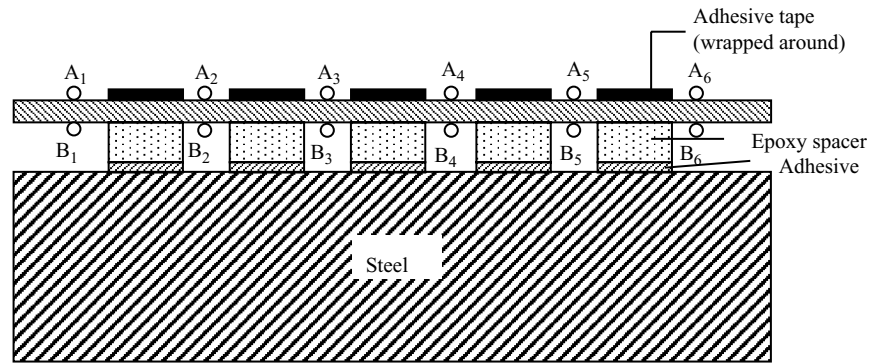


Fig. 6. Schematic of the edge of a composite and the specimen assembly for impact testing. A_1, A_2, A_3, A_4, A_5 and A_6 are contacts on one surface; B_1, B_2, B_3, B_4, B_5 and B_6 are contacts on the opposite surface. All the contacts are strips in the direction perpendicular to the length of the composite. Adhesive tape was wrapped around the entire assembly, including the steel plate, in regions away from the electrical contacts.

For the 24-lamina quasi-isotropic composite ($200 \times 20 \times 3.1$ mm), comparison was made after impact (at 0.73 and 3.63 J) between damage sensing by resistance measurement and by conventional ultrasonic inspection. For the resistance measurement, the electrical contact configuration was as shown in Fig. 2. For the ultrasonic inspection, the NovaScope 5000 instrument of NDT Systems, Inc., was used at a frequency of 12 MHz. The diameter of the active element (IBU15 transducer, mounted in a T300 Bubbler Tank) was 5.1 mm, with focusing down to 1.8 mm. Glycerin was used as the coupling agent. The active element was moved to various points on both the top and bottom surfaces. The points included one at the indentation area and one away from the indentation area.

3. Results and discussion

3.1. Eight-lamina unidirectional composite

Fig. 7 shows the surface resistance of the top (impact) side before and after impact at progressively increasing

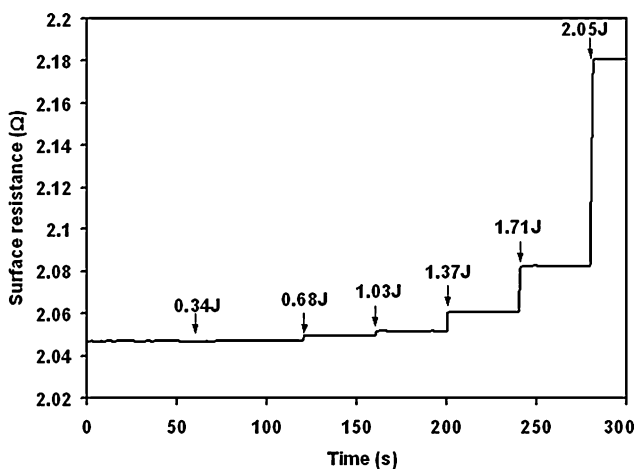


Fig. 7. Variation of the surface resistance of the top (impact) side upon impact damage at progressively increasing impact energy for the eight-lamina unidirectional composite tested using the configuration in Fig. 3.

levels of energy for the eight-lamina unidirectional composite tested using the configuration of Fig. 3. The resistance increased irreversibly, such that the resistance change increased with increasing impact energy. At an impact energy of 0.34 J, the damage, if any, was not detected. At an impact energy of 0.68 J or above, the damage was detected. The incremental change in resistance became larger as the impact energy increased, because the incremental increase in damage also became larger.

Fig. 8 shows the surface resistance of the top (impact) side before and after impact at progressively increasing levels of energy for the unidirectional composite tested using the configuration of Fig. 4. The result was similar to that obtained with the configuration of Fig. 3, but the extent of resistance change was quite small, except for the highest impact energy of 2.05 J. Thus, the sensing of minor damage is more effective when the electrical contacts are oblique to the fibers, at least in case of a unidirectional composite. The damage involved transverse separation between fibers. In the initial stage of damage, the length of the single crack corresponding to the transverse separation was about

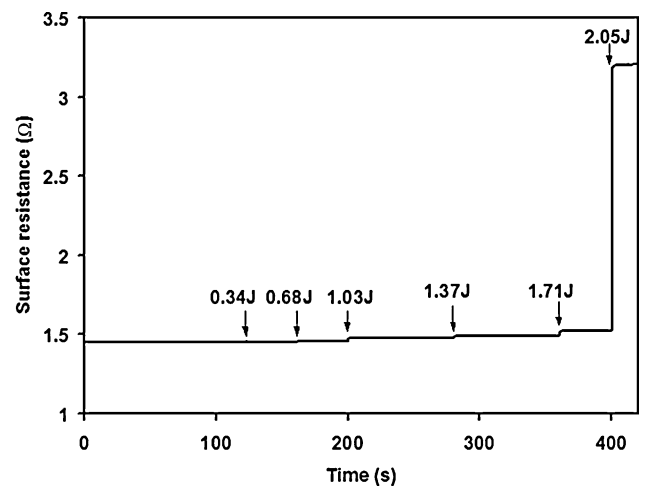


Fig. 8. Variation of the surface resistance of the top (impact) side upon impact damage at progressively increasing impact energy for the eight-lamina unidirectional composite tested using the configuration in Fig. 4.

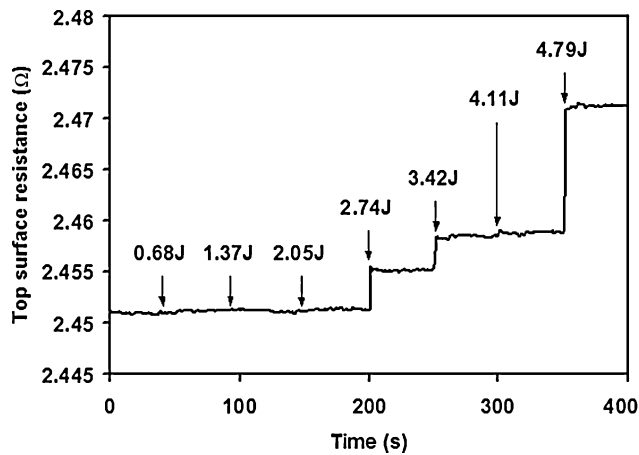


Fig. 9. Variation of the surface resistance of the top (impact) side upon damage at progressively increasing impact energy for the eight-lamina quasi-isotropic composite.

30 mm. In the later stage of damage, multiple cracks were observed and all the cracks increased in length gradually until failure occurred. Oblique contacts allow the electric current to have a component that is in the transverse direction, whereas contacts that are perpendicular to the fibers allow the electrical current to be in the longitudinal direction only. As a result, oblique contacts are more effective for damage sensing.

3.2. Eight-lamina quasi-isotropic composite

Fig. 9 shows the surface resistance of the top (impact) side of the eight-lamina quasi-isotropic composite before and after impact at progressively increasing levels of energy. Fig. 10 shows the corresponding result for the surface resistance of the bottom side. Fig. 11 shows the corresponding result for the oblique resistance.

The resistance increased with increasing impact energy for both top and bottom surfaces, such that the fractional

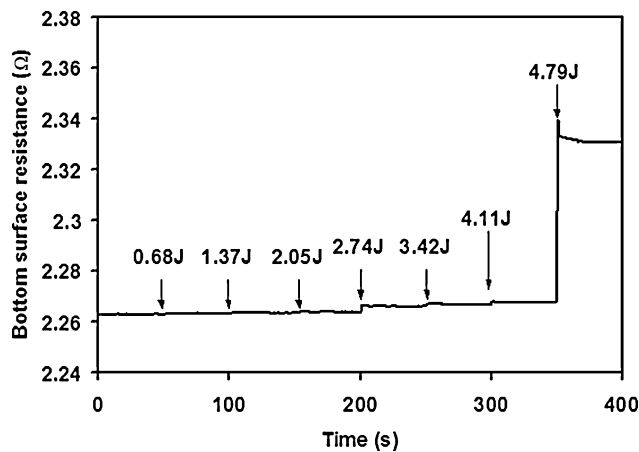


Fig. 10. Variation of the surface resistance of the bottom side upon damage at progressively increasing impact energy for the eight-lamina quasi-isotropic composite.

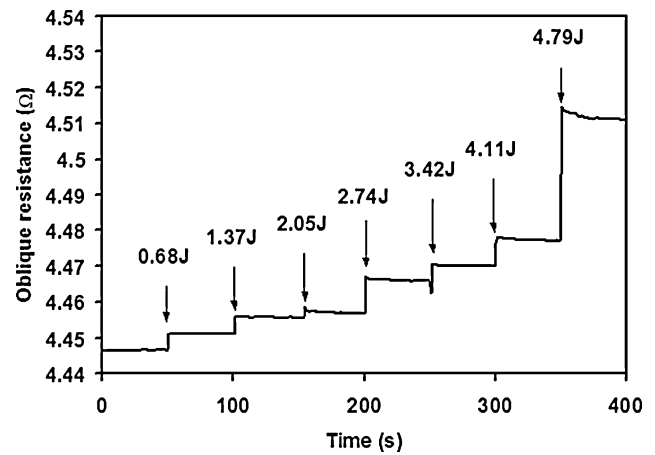


Fig. 11. Variation of the oblique resistance upon damage at progressively increasing impact energy for the eight-lamina quasi-isotropic composite.

change in resistance was less for the bottom surface. This is consistent with greater damage on the top surface than the bottom surface. In spite of the small thickness (1.0 mm) of the specimen, the degree of damage of the two opposite surfaces was clearly distinguished by the surface resistance measurement.

The oblique resistance also increased with increasing damage, but its fractional increase was even larger than that of the surface resistance of the top side. For example, after impact at 4.11 J, the fractional change in resistance is 0.32, 0.21 and 0.70% for the top surface resistance, bottom surface resistance and oblique resistance, respectively. The high sensitivity of the oblique resistance for damage is due to the sensitivity to interlaminar damage.

Table 1 shows the resistance and fractional change in resistance at various levels of impact energy for the top surface resistance, the bottom surface resistance and the oblique resistance. At any impact energy, the oblique resistance was higher than the top or bottom surface resistance. This is due to the fact that the oblique direction has a component in the through-thickness direction and the through-thickness resistivity is much higher than the longitudinal resistivity. The resistances of the top and bottom surfaces were close, though not equal.

For any of the three resistances measured, the resistance increased monotonically with increasing impact energy, as expected. Even the lowest impact energy of 0.68 J resulted in a measurable resistance increase.

The fractional increase in resistance was much larger for the oblique resistance than for the top or bottom surface resistance, except for the highest impact energy of 4.79 J. This is because delamination was the main type of damage and delamination affected the through-thickness resistance more than the longitudinal resistance. At the highest impact energy, the damage may involve some degree of interpenetration of the adjacent laminae and such damage would tend to decrease the through-thickness resistance.

Table 1
Resistance and fractional change in resistance at progressively increasing levels of impact energy for the eight-lamina quasi-isotropic composite

Impact energy (J)	Resistance (Ω)			Fractional change in resistance (%)		
	Top	Bottom	Oblique	Top	Bottom	Oblique
0	2.45096	2.26302	4.44648	0	0	0
0.68	2.45120	2.26329	4.45128	0.00996	0.01161	0.10863
1.37	2.45130	2.26360	4.45575	0.01392	0.02529	0.20910
2.05	2.45136	2.26383	4.45725	0.01644	0.03567	0.24296
2.74	2.45514	2.26618	4.46623	0.17049	0.13928	0.44484
3.42	2.45841	2.26683	4.47027	0.30413	0.16829	0.53584
4.11	2.45872	2.26773	4.47760	0.31658	0.20811	0.70070
4.79	2.47127	2.33156	4.51215	0.82883	3.02862	1.47758

Table 2 shows the diameter of the indentation on the top surface of the laminate after each level of impact damage, such that the impact at different energies was directed at different points on the top surface of the laminate. Both the diameter and depth increased monotonically with increasing impact energy. The depth ranged from 7 to 26% of the specimen thickness.

3.3. 24-Lamina quasi-isotropic composite

Fig. 12 and Table 3 show the variation of resistance with impact energy for the 24-lamina quasi-isotropic composite. For each segment, the oblique resistance, the top surface resistance and the bottom surface resistance were shown in Fig. 12(a)–(c), respectively.

The resistance increased with increasing impact energy, such that the resistance increase was abrupt at an impact energy between 2.18 and 2.90 J. The oblique resistance increase was monotonic, but the top and bottom surface resistances did not increase monotonically in all cases. The behavior was most complex for the bottom resistance. Thus, the oblique resistance is a most reliable indicator of damage. The fractional increase in oblique resistance was lower for the right and left segments than the middle segment, due to more significant damage in the middle segment.

Figs. 12–15 show the variation of the fractional change in resistance with the impact energy for the top surface resistance, bottom surface resistance, oblique resistance and

$L + M + R$ resistance, respectively. In each of Figs. 12–14, the curves for L , M , R and $L + M + R$ are shown. In Fig. 15, the curves for the top surface resistance, bottom surface resistance and oblique resistance are shown. In Figs. 12–14, the middle (M) segment is associated with the highest fractional change in resistance at the same impact energy, since the point of impact is in the M segment; the $L + M + R$ segment is associated with higher fractional change in resistance than the right (R) or left (L) segments, since the point of impact is in the M segment.

The differences among the curves in the same figure are smaller in Fig. 14 (oblique resistance) than in Fig. 12 (top surface resistance) or Fig. 13 (bottom surface resistance). This is because of the oblique resistance reflecting the interior condition more than the top or bottom surface resistance, and the interior condition being less dramatically changed than the surface condition upon impact.

In Fig. 15 ($L + M + R$), the oblique resistance shows larger fractional change in resistance than the top or bottom surface resistance at the same impact energy. This is due to the sensitivity of the oblique resistance to the interior condition. In Fig. 15, the fractional change in the bottom surface resistance is slightly higher than the fractional change in the top surface (impact surface) resistance for the same impact energy above 2 J. This is probably due to the interior damage in the specimen. Due to the large scale in

Table 2
Diameter and depth of the indentation at various levels of impact energy for the eight-lamina quasi-isotropic composite

Impact energy (J)	Diameter (mm)	Calculated depth (mm)
0.68	2.3	0.07
1.37	2.9	0.11
2.05	3.0	0.12
2.74	3.3	0.14
3.42	3.7	0.18
4.11	4.2	0.23
5.78	4.4	0.26

The impact at different energies was directed at different points on the top surface of the composite.

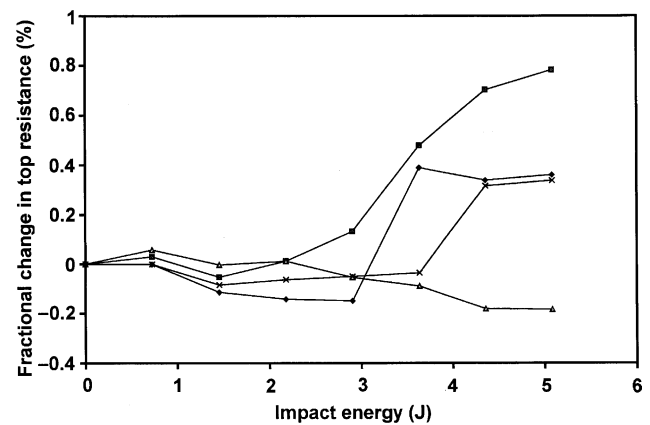


Fig. 12. Variation of the fractional change in top surface resistance with impact energy for L (♦), M (■), R (△) and $L + M + R$ (×) segments.

Table 3
Resistance (Ω) after impact at progressively increasing energy for the 24-lamina quasi-isotropic composite

Impact energy (J)	Top			Bottom			Oblique			L+M+R		
	L	M	R	L	M	R	L	M	R	Top	Bottom	Oblique
0	0.67356	0.65167	0.56660	0.57710	0.54475	0.73343	7.65152	7.24330	7.07294	1.89116	1.85438	8.08806
0.73	0.67346	0.65174	0.56656	0.57703	0.54463	0.73320	7.65477	7.24684	7.07623	1.89072	1.85382	8.09048
1.45	0.67295	0.65173	0.56664	0.57671	0.54540	0.73300	7.66159	7.25429	7.08310	1.89098	1.85420	8.09879
2.18	0.67285	0.65206	0.56662	0.57666	0.54560	0.73289	7.66500	7.25767	7.08632	1.89073	1.85414	8.10076
2.90	0.67490	0.65432	0.56781	0.57781	0.54666	0.73614	7.70092	7.29206	7.11912	1.89119	1.85453	8.11784
3.63	0.67461	0.65509	0.56782	0.57749	0.54828	0.73614	7.70612	7.29795	7.12419	1.89640	1.86024	8.14234
4.36	0.67423	0.65518	0.56767	0.57711	0.54857	0.73595	7.70815	7.30043	7.12615	1.89654	1.86096	8.14616
5.08	0.67415	0.65545	0.56767	0.57665	0.54926	0.73560	7.71474	7.30722	7.13264	1.89645	1.86115	8.15073

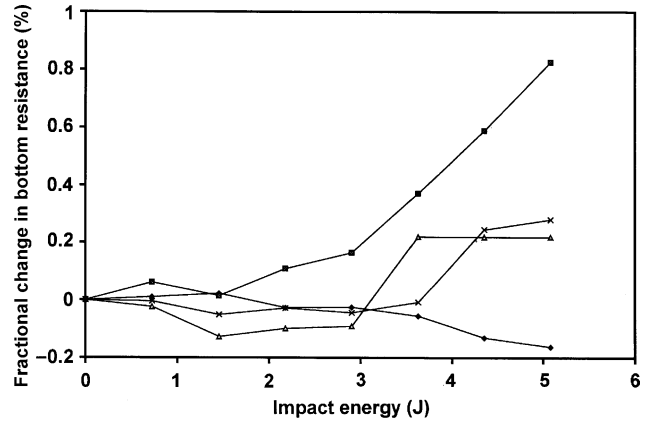


Fig. 13. Variation of the fractional change in bottom surface resistance with impact energy for L (◆), M (■), R (△) and L+M+R (×) segments.

practical structures, the case in Fig. 15 (L+M+R) is most relevant to practical application.

The sum of the top surface resistances of the L, M and R segments (1.892–1.897 Ω , Table 3) is similar to the measured L+M+R top surface resistance (1.891–1.897 Ω , Table 3). This consistency confirms the reliability of the four-probe method used. The sum of the bottom surface resistances of the L, M and R segments (1.822–1.834 Ω , Table 3) is similar to the measured L+M+R bottom surface resistance (1.854–1.861 Ω , Table 3). However, the sum of the oblique resistances of the L, M and R segments (14.89–15.02 Ω , Table 3) is considerably higher than the measured L+M+R oblique resistance (8.09–8.15 Ω , Table 3), because the degree of obliqueness is lower for L+M+R than for L, M or R individually and a lower resistance is associated with a lower degree of obliqueness.

Table 4 shows the diameter of the indentation on the top surface of the laminate after each level of impact damage. The depth range from 0.3 to 6% of the specimen thickness of 3.2 mm.

Fig. 16 shows the variation of the oblique resistance upon impact at 0.73 and 3.63 J, respectively. The fractional change in oblique resistance upon impact was 0.0255 and

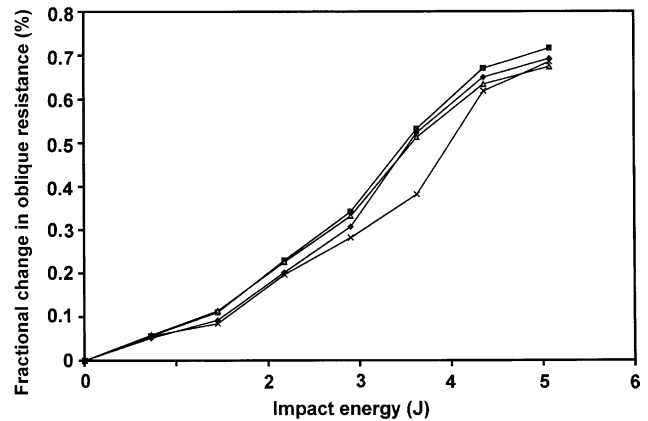


Fig. 14. Variation of the fractional change in oblique surface resistance with impact energy for L (◆), M (■), R (△) and L+M+R (×) segments.

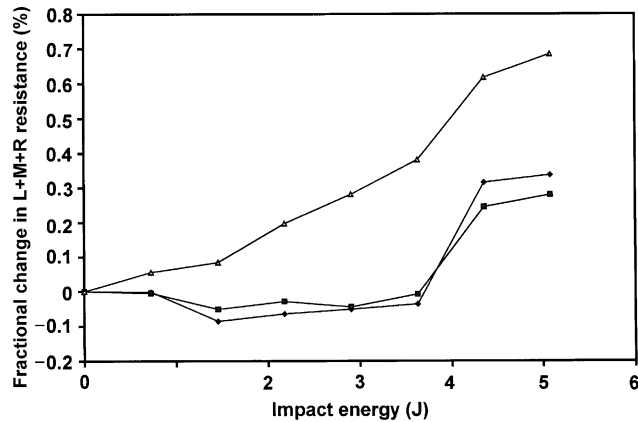


Fig. 15. Variation of the fractional change in $L+M+R$ resistance with impact energy for top surface resistance (◆), bottom surface resistance (■) and oblique resistance (△).

0.0756% for impact at 0.73 and 3.63 J, respectively. Hence, a higher impact was associated with a higher fractional change in resistance, as expected. For the lower impact energy of 0.73 J, the top and bottom surface resistances did not change upon impact, whereas the oblique resistance did. For the higher impact energy of 3.63 J, the top and bottom surface resistances changed upon impact by 0.105 and 0.0192%, respectively. Although the fractional change was larger for the top surface resistance than the oblique resistance upon impact at the higher energy, the signal-to-noise ratio was higher for the oblique resistance. Therefore, with results at both impact energies considered, it is clear that the oblique resistance is the best indicator.

Internal damage (such as delamination and matrix cracking) probably occurred to a limited extent, but it could not be observed at the surface of the composite. This subtlety of the internal damage is consistent with the small depth of indentation. In spite of the subtlety, the internal damage was revealed by electrical resistance measurement. Because of the absence of internal damage observation, quantitative relationship between the fractional change in resistance and the damage state could not be determined.

Damage at the bottom side was visible for the 8-lamina composite at impact energy above 3 J. It was not visible for

Table 4

Diameter and depth of the indentation at various levels of impact energy for the 24-lamina quasi-isotropic composite

Impact energy (J)	Diameter (mm, ± 0.2)	Calculated depth (mm)
0.73	1.0	0.01
1.45	1.6	0.03
2.18	2.1	0.06
2.90	2.5	0.08
3.63	2.9	0.11
4.36	3.4	0.15
5.08	3.9	0.20

The impact was directed at different points on the top surface of the composite.

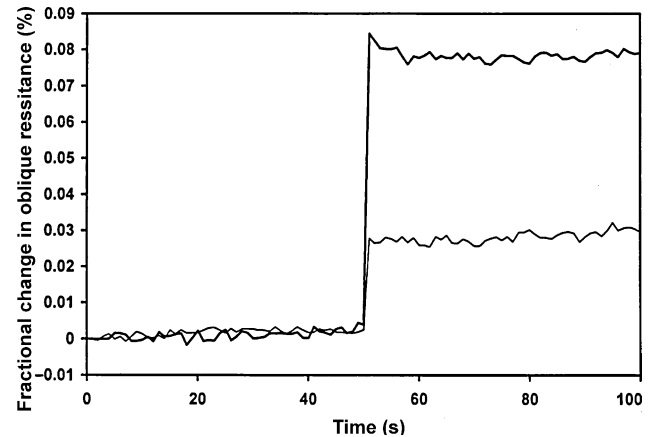


Fig. 16. Variation of the fractional change in oblique resistance upon impact at 0.73 J (thin curve) and at 3.63 J (thick curve).

the 24-lamina composite at any of the impact energy levels used. In spite of the absence of visible damage at the bottom side of the 24-lamina composite, the minor damage at the bottom side was detected by electrical resistance measurement.

Interaction of damage with the free edges of the 10-mm wide specimen was not observed. This is consistent with the small diameter of the indentation.

Comparison of the results in Figs. 15 and 16 (thick curve) for the impact energy of 3.63 J shows that the fractional change in oblique resistance was lower by a factor of 5 in Fig. 16 (thick curve) (0.08%, single-impact damage) than in Fig. 15 (0.4%, cumulative damage). This difference is partly caused by the 20-mm width of the specimen of Fig. 16 (thick curve), compared to the 10-mm width of the specimen of Fig. 15. Indeed, for the impact energy of 0.73 J, comparison of Figs. 15 and 16 (thin curve) (both single-impact damage for 0.73 J) shows that the fractional change in oblique resistance was lower by a factor of 2 for Fig. 16 (thin curve) than Fig. 15.

Ultrasonic inspection failed to detect the damage for the low impact energy of 0.73 J. The ultrasonic signal was the same at the indentation and away from the indentation, whether the active element was on the top surface or the bottom surface. For the high impact energy of 3.63 J, delamination was detected, as shown by the echo from the interface due to the delamination. This interface was located at a depth of 1/4 of the thickness of the laminate, as measured from the top (impact) side. The delamination was detected with the active element on the bottom side, but it was not detected with the active element on the top side. For any position of the active element, for both impact energies, the ultrasonic inspection was partly obscured by noise (known as ringing) that was due to the interlaminar interfaces that were inherent in the laminate. This noise significantly reduced the sensitivity of the ultrasonic technique for damage detection. Due to the limited sensitivity, the size of the delamination could not be determined.

3.4. General comments

Comparison of damage sensing by resistance measurement and that by ultrasonic inspection shows that the former is more sensitive, particularly when the damage is minor. On the other hand, ultrasonic inspection can give information on the depth of the delamination, whereas the resistance method cannot.

This paper provides a basic one-dimensional study of the technique of composite damage sensing by resistance measurement. Extension of the study to two dimensions is the subject of a separate paper. The extension involves the use of a two-dimensional array of electrical contacts, each of which can be in the form of a circle, a rectangle or other shapes.

In general, whether the number of dimensions is 1 or 2, the sensitivity and spatial resolution of damage detection improve with decreasing spacing between the adjacent voltage contacts. Furthermore, the sensitivity increases with the current used.

4. Conclusion

Drop impact (energy up to 5 J) damage of continuous carbon fiber epoxy–matrix composite laminates (quasi-isotropic and unidirectional) was studied by electrical resistance measurement (four-probe method, with electrical contacts on the surface). The oblique resistance at an angle between the longitudinal and through-thickness directions, as measured by using electrical contacts that were not directly opposite each other on the two opposite sides of the laminate, was more effective than the surface longitudinal resistance in indicating damage, particularly interior damage. However, the surface longitudinal resistance of the top (impact) side and that of the bottom side were also effective. In the case of a unidirectional laminate, electrical contacts directed at an angle of 45° to the fiber direction in the plane of the laminate were more effective than those that were perpendicular to the fiber direction. The resistance measurement was sensitive to even minor damage, which was associated with negligible indentation by the drop impact. It was also sensitive to damage in the region not containing the indentation. Furthermore, it was able to distinguish between the greater damage in the region containing the indentation from the smaller damage in the adjacent region not containing the indentation, thus allowing spatial distribution sensing. On the other hand, the oblique resistance suffers from the values of adjacent longitudinal segments of the composites being not additive, i.e. the sum of the values of the individual segments being greater than the value of the totality of the segments. In contrast, the top and bottom surface resistances are additive.

The resistance method is more sensitive than the ultrasonic method for carbon fiber composite damage detection. Upon impact at 0.73 J, the ultrasonic method used in this work failed to detect the damage, but the increase of the oblique resistance indicated the damage.

Acknowledgement

This work was supported in part by the U.S. National Science Foundation.

References

- [1] Sjogren A, Krasnikovs A, Varna J. Experimental determination of elastic properties of impact damage in carbon fibre/epoxy laminates. *Composites Part A* 2001;32(9):1237–42.
- [2] de Freitas M, Silva A, Reis L. Numerical evaluation of failure mechanisms on composite specimens subjected to impact loading. *Composites Part B* 2000;31(3):199–207.
- [3] Sohn MS, Hu XZ, Kim JK. Fractography of damaged carbon fiber/epoxy composites after low-velocity impact. *Mech Corros Prop, Ser A (Key Eng Mater)* 2000;183:1177–82.
- [4] Sohn MS, Hu XZ, Kim JK, Walker L. Impact damage characterization of carbon fibre/epoxy composites with multi-layer reinforcement. *Composites Part B* 2000;31(8):681–91.
- [5] Sohn MS, Hu XZ, Kim JK. Impact damage resistance of carbon fibre/epoxy composites laminates containing short Kevlar fibres. *Polym Polym Compos* 2001;9(3):157–568.
- [6] Kwon OY, Jun JK, Dzenis YA. Nondestructive methods for the damage assessment of cylindrically curved composite laminates subjected to low-velocity impact. *Am Soc Mech Eng (Publ) NDE* 2002;23:5–10.
- [7] Antonov AV, Zelenskii ES, Kuperman AM. Impact resistance of reinforced plastics based on polysulfone-epoxy blends. *J Reinf Plast Compos* 2003;22(4):361–72.
- [8] Belingardi G, Vadori R. Influence of the laminate thickness in low velocity behavior of composite material plate. *Compos Struct* 2003; 61(1–2):27–38.
- [9] Ochola RO, Marcus K, Nurick GN, Franz T. Mechanical behaviour of glass and carbon fibre reinforced composites at varying strain rates. *Compos Struct* 2004;63(3–4):455–67.
- [10] Kusaka T, Hojo M, Ochiai S, Kurokawa T. Rate-dependent mode II interlaminar fracture behavior of carbon-fiber/epoxy composite laminates. *Mater Sci Res Int* 1999;5(2):98–103.
- [11] Kusaka T. Experimental characterization of interlaminar fracture behavior in polymer matrix composites under low-velocity impact loading. *JSME Int J Ser A* 2003;46(3):328–34.
- [12] Morioka K, Tomita Y. Effect of lay-up sequences on mechanical properties and fracture behavior of CFRP laminate composites. *Mater Charact* 2000;45(2):125–36.
- [13] Wang S, Chung DDL. Mechanical damage in carbon fiber polymer-matrix composite, studied by electrical resistance measurement. *Compos Interfaces* 2002;9(1):51–60.
- [14] Chung DDL, Wang S. Self-sensing of damage and strain in carbon fiber polymer–matrix structural composites by electrical resistance measurement. *Polym Polym Compos* 2003;11(7):515–25.
- [15] Wang X, Chung DDL. Fiber breakage in polymer-matrix composite during static and dynamic loading, studied by electrical resistance measurement. *J Mater Res* 1999;14(11):4224–9.
- [16] Wang X, Wang S, Chung DDL. Sensing damage in carbon fiber and its polymer–matrix and carbon–matrix composites by electrical resistance measurement. *J Mater Sci* 1999;34(11):2703–14.
- [17] Wang X, Chung DDL. Self-monitoring of fatigue damage and dynamic strain in carbon fiber polymer–matrix composite. *Composites Part B* 1998;29B(1):63–73.
- [18] Wang X, Chung DDL. Sensing delamination in a carbon fiber polymer–matrix composite during fatigue by electrical resistance measurement. *Polym Compos* 1997;18(6):692–700.
- [19] Wang S, Chung DDL. Piezoresistivity in continuous carbon fiber polymer–matrix composite. *Polym Compos* 2000;21(1):13–19.